Publishing House
AKAPIT

COMPUTER METHODS IN MATERIALS SCIENCE
Informatyka w Technologii Materiałów

Vol. 18, 2018, No. 1

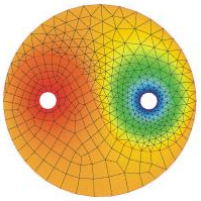

APPLICATION OF THE IMMUNE ALGORITHM IRM FOR SOLVING THE INVERSE PROBLEM OF METAL ALLOY SOLIDIFICATION INCLUDING THE SHRINKAGE PHENOMENON

ADAM ZIELONKA*, EDYTA HETMANIOK, DAMIAN SŁOTA

Institute of Mathematics, Silesian University of Technology
Kaszubska 23, 44-100 Gliwice, Poland
**Corresponding author: adam.zielonka@polsl.pl*

Abstract

In the paper the mathematical model of the inverse one-dimensional problem of binary alloy solidification, with the material shrinkage phenomenon taken into account, is defined. The process is described by using the model of solidification in the temperature interval, whereas the shrinkage of material is modeled basing on the mass balance equation. The inverse problem consists in reconstruction of the heat transfer coefficient on the boundary of the casting mould separating the cast from the environment. Lack of this data is compensated by the measurements of temperature in the control point located inside the mould. The method of solving the investigated problem is based on two procedures: the implicit scheme of finite difference method supplemented by the procedure of correcting the field of temperature in the vicinity of liquidus and solidus curves and the immune optimization algorithm IRM.

Key words: Solidification, Binary Alloy, Material shrinkage, Immune algorithm

1. INTRODUCTION

The problems describing the physical, technical or engineering processes can be divided into two general groups: direct problems (Sczygiol & Dyja, 2007; Sowa & Bokota, 2007; Piekarska et al., 2011), when all the input data are given for the start, and the inverse problems, when some part of the input data is unknown, so the goal of such task is to reconstruct the missing elements on the basis of some additional information concerning the effects caused by the process (Alifanov, 1994; Beck & Blackwell, 1988). Solving the inverse problem is much more difficult than solving the direct problem, but in return we get the possibility of determining the values of coefficients which cannot be directly measured or designing the problems in which the initial or boundary conditions or the values of parameters are selected such that they ensure a required run of the process. The inverse problem provides a very useful tool for analyses of various processes (see for example Hojny & Głowacki, 2009; Szeliga et al., 2004, Talar et al., 2002; Telejko & Malinowski, 2004).

An object of this research is the binary alloy solidification process including the phenomenon of creating the air gap between the cast and the mould. This phenomenon is the result of the metal shrinkage caused by the different densities of the liquid and solid states. This kind of problem was already investigated by some authors. For example, Nawrat et al. (2009) determined the heat conduction coefficient of the gap on the basis of temperature measurements in the crystallizer walls. They investigated the heat resistance of the air gap created between the ingot and crystallizer in the continuous casting process and for modeling this process they used the Stefan problem. Thermal resistance of the

 ISSN 1641-8581

gap between the mould, or the crystallizer, and the ingot was also determined in other papers (Shestakov et al., 1994) as well as the interfacial heat transfer coefficient between the form and the cast (Cheung et al., 2009; O'Mahoney & Browne, 2000). Matlak and Słota (2015) considered the shrinkage of metal occurring in the pure metal solidification modeled by means of the one-dimensional Stefan problem, whereas authors of the current paper (Hetmaniok et al., 2017) tested the solution technique for solving the direct problem of the alloy solidifying within the casting mould with the air gap effect and they described the examined process by means of the solidification in the temperature interval.

In this paper we investigate the mathematical model of the inverse one-dimensional problem of the binary alloy solidification, with the material shrinkage phenomenon taken into account. The process is described by using the model of solidification in the temperature interval. In this case we deal with the heat conduction equation with the source element enclosed including the latent heat of fusion and the volumetric contribution of the solid phase (Majchrzak & Mochnacki, 1995; Mochnacki & Suchy, 1995). The shrinkage of metal is modeled basing on the mass balance equation. The inverse problem consists in reconstruction of the heat transfer coefficient on the boundary of the casting mould separating the cast from the environment. Lack of this data is compensated by the measurements of temperature in the control point located in the middle of the mould. For solving the inverse problem one of the optimization algorithms, the IRM algorithm, developed on the basis of the immune system functioning in the mammal bodies is used (Bersini &Varela, 1991; Hetmaniok et al., 2012). The elaboration contains the results of numerical research executed for various levels of input data perturbations and for measurements generated in series with the constant, but different for every series, time step. Authors of the current paper discussed already the similar approach, but by applying the Artificial Bee Colony algorithm (Zielonka et al., 2017). Encouraged by the promising results we decided to use in this approach another algorithm based on the biological inspirations, that is the immune algorithm, to check how this optimization procedure deals with such task. In general, the artificial intelligence algorithms inspired by nature are widely applied in solving the problems requiring optimization because of their effectiveness connected with relative simplicity and easiness of implementation. Since we plan in future to solve more advanced problems, concerning the identification of more parameters in two or three-dimensional domains, we test the usefulness of biologically inspired algorithms in solving the problems of considered kind.

2. GOVERNING EQUATIONS

In figure 1 there is presented the solidifying plate of thickness $d(t)$, width h and height l ($d(t) << h$ and $d(t) << l$). Region $\Omega = \{(x,t) : x \in (0, d(t)),\ t \in (0, t^*)\}$ of solidifying material is divided into three subregions: occupied by the liquid phase, mushy zone (two-phase zone combining liquid and solid phases) and solid phase. As figure 1 shows, the region Ω of the cast is bounded by the region $\Omega_m = \{(x,t) : x \in (d_0, b),\ t \in (0, t^*)\}$ of the casting mould and both regions are separated by the air gap created and increased during the solidification process. So, at the begining of solidification $d(0) = d_0$ and next, while the solidification process goes on, the boundary $d(t)$ of the cast moves by forming the air gap.

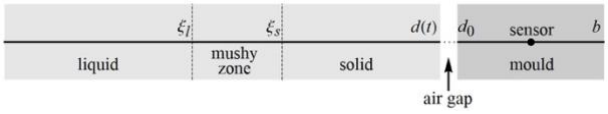

***Fig. 1**. Region of the problem*

The distribution of temperature in region Ω is described by the following heat conduction equation

$$c\rho \frac{\partial T(x,t)}{\partial t} + v_x \frac{\partial T(x,t)}{\partial x} = \lambda \frac{\partial^2 T(x,t)}{\partial x^2} + L\rho \frac{\partial f_s(x,t)}{\partial t}, \quad (1)$$

where c, ρ and λ denote the specific heat, mass density and thermal conductivity coefficient, respectively, v_x describes the velocity vector, L is the latent heat of solidification, f_s means the volumetric solid state fraction and, finally, T is the temperature, t describes the time and x refers to the spatial variable. In this approach we neglect the natural convection in the liquid phase, as well as the strain energy of the mushy zone and since the volumetric solid state fraction f_s depends on the temperature we can write this function in the following way

$$\frac{\partial f_s}{\partial t} = \frac{\partial f_s}{\partial T}\frac{\partial T}{\partial t}. \tag{2}$$

Including the above relation into equation (1) we get the equation describing the heat conduction in the homogeneous region including the solid phase, mushy zone and liquid phase, that is for all $(x,t) \in \Omega$:

$$C\rho\frac{\partial T(x,t)}{\partial t} + v_x\frac{\partial T(x,t)}{\partial x} = \lambda\frac{\partial^2 T(x,t)}{\partial x^2}, \tag{3}$$

where $C = c - L\frac{\partial f_s}{\partial T}$ defines the substantial thermal capacity. Function f_s can be the linear function depending on temperature (Majchrzak & Mochnacki, 1995; Mochnacki & Suchy, 1995) in the mushy zone. Thus, since it must be fulfilled that $f_s(T_L) = 0$ and $f_s(T_S) = 1$, where T_L and T_S denote the liquidus and solidus temperatures, we assume the following form of function describing the volumetric solid state fraction

$$f_s(T) = \frac{T_L - T}{T_L - T_S} \tag{4}$$

for $T \in [T_L, T_S]$. Taking into account function (4), the substantial thermal capacity is defined in dependence on temperature as follows

$$C = \begin{cases} c_l, & T > T_L, \\ c_{mz} + \dfrac{L}{T_L - T_S}, & T \in [T_L, T_S], \\ c_s, & T < T_S, \end{cases} \tag{5}$$

where c_l, c_{mz} and c_s denote the specific heat of liquid phase, mushy zone and solid phase, respectively. The thermal conductivity coefficient and the density, occurring in equation (3), depend also on temperature, so we have

$$\lambda = \begin{cases} \lambda_l, & T > T_L, \\ \lambda_{mz}, & T \in [T_L, T_S], \\ \lambda_s, & T < T_S \end{cases} \text{ and } \rho = \begin{cases} \rho_l, & T > T_L, \\ \rho_{mz}, & T \in [T_L, T_S], \\ \rho_s, & T < T_S. \end{cases} \tag{6}$$

Since the mushy zone is a two-phase zone in which both phases, liquid and solid, coexist, we express the specific heat, thermal conductivity coefficient and density in the mushy zone as depending on the volumetric solid state fraction f_s in the following way

$$c_{mz} = c_l(1 - f_s) + c_s f_s,$$

$$\lambda_{mz} = \lambda_l(1 - f_s) + \lambda_s f_s \quad \text{and}$$

$$\rho_{mz} = \rho_l(1 - f_s) + \rho_s f_s. \tag{7}$$

In mould region Ω_m the temperature is distributed according to the following heat conduction equation

$$c_m\rho_m\frac{\partial T_m(x,t)}{\partial t} = \lambda_m\frac{\partial^2 T_m(x,t)}{\partial x^2}, \tag{8}$$

where T_m denotes the temperature of the casting mould and c_m, ρ_m, λ_m are the specific heat, mass density and thermal conductivity coefficient of the material, the casting mould is made of.

Equations (3) and (8) are completed by the following initial and boundary conditions. At the beginning of the process we have

$$T(x,0) = T_0(x) \quad \text{for} \quad x \in [0, d_0]$$

and

$$T_m(x,0) = T_{m,0}(x) \quad \text{for} \quad x \in [d_0, b], \tag{9}$$

where $T_0(x) > T_L$ because for $t = 0$ the cast is in the liquid state. To satisfy the consistency condition we assume that $T_0(d_0) = T_{m,0}(d_0)$. Moreover we have

$$-\lambda \frac{\partial T(0,t)}{\partial x} = 0$$

and (10)

$$-\lambda_m \frac{\partial T_m(b,t)}{\partial x} = \alpha (T_m(b,t) - T_\infty) \text{ for } t \in (0,t^*),$$

where α denotes the heat transfer coefficient and T_∞ describes the temperature of environment. In contact zone of the cast and the casting mould we assume the fourth kind boundary condition in two forms: at the beginning of the process there is a perfect contact between the cast and the mould

$$-\lambda \frac{\partial T(d_0,t)}{\partial x} = -\lambda_m \frac{\partial T_m(d_0,t)}{\partial x} \tag{11}$$

and next, when the air gap between the cast and the mould starts to occur, we assume the condition

$$-\lambda_s \frac{\partial T(d(t),t)}{\partial x} = \frac{T(d(t),t) - T_m(d_0,t)}{R} = -\lambda_m \frac{\partial T_m(d_0,t)}{\partial x}, \tag{12}$$

where $R = \dfrac{d_0 - d(t)}{\lambda_g}$ describes the thermal resistance with λ_g denoting the thermal conductivity coefficient of the air gap. Width $d(t)$ of the cast depends on time and to determine $d(t)$ we use the mass balance equation

$$m_0 = m_l + m_{mz} + m_s, \tag{13}$$

according to which the total mass of the material m_0 (constant in the modeled solidification process) must be equal to the sum of masses of the material in the liquid, intermediate (mushy zone) and solid states. Using the notation from figure 1, equation (13) can be formulated in the following form

$$\rho_l d_0 hl = \rho_l \xi_l hl + \rho_{mz}(\xi_s - \xi_l)hl + \rho_s (d(t) - \xi_s)hl. \tag{14}$$

Hence we get

$$d(t) = \xi_s + \frac{\rho_l}{\rho_s}(d_0 - \xi_l) - \frac{\rho_{mz}}{\rho_s}(\xi_s - \xi_l). \tag{15}$$

Dependence on time is expressed here by the values ξ_l and ξ_s denoting the locations of T_L and T_S, that is the boundaries of the mushy zone changing in time.

Before the solid state occurs in the process, only the liquid state and mushy zone are taken into account, so the mass balance equation has the form

$$m_0 = m_l + m_{mz}. \tag{16}$$

According to the notation from figure 1, equation (16) can be presented in the form

$$\rho_l d_0 hl = \rho_l \xi_l hl + \rho_{mz}(d(t) - \xi_l)hl \tag{17}$$

and hence, the width $d(t)$ before occurance of the solid state is expressed by formula

$$d(t) = \xi_l + \frac{\rho_l}{\rho_{mz}}(d_0 - \xi_l). \tag{18}$$

In the above equations there is one unknown element: the heat transfer coefficient α of the casting mould material included in one of the boundary conditions (10). Thus, the considered inverse problem consists in reconstruction of this coefficient and in determination of the temperature distribution in the entire investigated region, that is in the cast and in the mould, on the ground of the measurements of temperature read from the sensor located in the middle of the mould as it is presented in figure 1.

For the known value of coefficient α the problem turns into the direct solidification problem with the air gap created between the cast and the mould. Thus, by solving this problem we are able to calculate the values of temperature $T_{m,i} = T_m(x,t_i)$ in the middle point x of the mould, where the thermocouple is located, corresponding with the assumed form of coefficient α. Then, by using the measurements of temperature U_i, for $i = 1,\ldots,N$, we define the functional

$$J(\alpha) = \sum_{i=1}^{N} (T_{m,i} - U_i)^2 \tag{19}$$

representing the error of approximate solution $T_{m,i}$. On the way of minimizing this functional we select such value of the heat transfer coefficient α that the reconstructed values of temperature are the

closest as possible to the measured values. The method of solution is based on two procedures: one procedure serves for solving the direct problem and the second one is used for minimizing functional (19).

3. SOLUTION OF THE DIRECT PROBLEM

To solve the direct problem, associated to the investigated inverse problem, we use the implicit scheme of the finite difference method supplemented by the procedure of correcting the field of temperature in the vicinity of liquidus and solidus curves (Majchrzak & Mochnacki, 1995; Mochnacki & Suchy, 1995). To apply this method we impose two different meshes: one (with the nodes located more densely) in the cast region and another one in the mould region. The last node of the cast region is always located at point $d(t)$, therefore, when the air gap starts to grow in result of solidification, the last node of the cast region moves.

The idea of the used method assumes the correction of the calculated value of temperature in the given node in case of the phase change. Let us suppose that node x_i in moment t_p is in the liquid phase, which means that its temperature satisfies the condition $T_i^p > T_L$. To calculate the value of temperature in the next step t_{p+1} we use then the parameters appropriate to the liquid phase. If the calculated new temperature satsifies still the condition $T_i^{p+1} > T_L$, it means that the phase did not change in node x_i and the temperature has the correct value. In opposite case, that is when $T_i^{p+1} \in (T_S, T_L]$, the calculated value of temperature must be corrected, because apparently the phase changed within the period of time $\Delta t = t_{p+1} - t_p$, so for part of this time the values of parameters adequate to new phase – mushy zone - should be used for calculations in node x_i.

To determine this correction we use the energy balance relation for the control volume V_i with central point x_i. The decrease of temperature from value T_i^p to value T_i^{p+1} causes the following change of the enthalpy

$$\Delta H_i = C_l \rho_l (T_i^p - T_i^{p+1}) \Delta V_i , \tag{20}$$

where C_l and ρ_l describe the substantial thermal capacity and density of the liquid phase. The decrease of temperature can be presented as the sum of two processes: cooling from value T_i^p to the liquidus temperature T_L and from liquidus temperature T_L to the required value $\tilde{T}_i^{p+1}$:

$$\Delta H_i = C_l \rho_l (T_i^p - T_L) \Delta V_i + C_{mz} \rho_{mz} (T_L - \tilde{T}_i^{p+1}) \Delta V_i , \tag{21}$$

where C_{mz} and ρ_{mz} describe the substantial thermal capacity and density of the mushy zone. Thus, from equations (20)-(21) we derive the formula for the corrected value of temperature in node x_i:

$$\tilde{T}_i^{p+1} = T_L - \frac{C_l \rho_l}{C_{mz} \rho_{mz}} (T_L - T_i^{p+1}) . \tag{22}$$

In similar way we receive the formula for the corrected value of temperature in case when node x_i changes the phase from the mushy zone to the solid phase

$$\tilde{T}_i^{p+1} = T_S - \frac{C_{mz} \rho_{mz}}{C_s \rho_s} (T_S - T_i^{p+1}) , \tag{23}$$

with C_s and ρ_s denoting the substantial thermal capacity and density of the solid phase. In our approach we do not consider the change of temperature in node x_i from the value $T_i^p > T_L$ to the value $T_i^{p+1} < T_S$. We select the time step so that we can avoid such situation.

After determining the value of temperature in node x_i we calculate the contribution of the solid phase in this node by using formula (4) and the locations of points ξ_l and ξ_s bounding the intermediate (mushy) zone. To determine the location of point ξ_l we need to find the nodes x_{i-1} and x_i for which $T_{i-1}^{p+1} > T_L$ and $T_i^{p+1} < T_L$, determine the line going through points (x_{i-1}, T_{i-1}^{p+1}) and (x_i, T_i^{p+1}) and find the point at which the line takes the value T_L. In this way we obtain

$$\xi_l = x_{i-1} + \frac{x_{i-1} - x_i}{T_{i-1}^{p+1} - T_i^{p+1}} (T_L - T_{i-1}^{p+1}) . \tag{24}$$

Similarly, only now by taking the nodes x_{j-1} and x_j for which $T_{j-1}^{p+1} > T_S$ and $T_j^{p+1} < T_S$, we get

$$\xi_s = x_{j-1} + \frac{x_{j-1} - x_j}{T_{j-1}^{p+1} - T_j^{p+1}} (T_S - T_{j-1}^{p+1}). \qquad (25)$$

One step of calculations finishes the determination of the cast width $d(t)$ with the aid of formula (15) or (18).

4. IMMUNE RECRUITMENT MECHANISM

Minimization of functional (19) is realized by using the Immune Recruitment Mechanism, that is the immune optimization algorithm inspired by the mechanisms functioning in the immunological systems of living organisms (Bersini & Varela, 1991; Hetmaniok et al., 2012). The main elements participating in the defensive reaction of the system are the white blood cells, called the lymphocytes. In presence of the dangerous antigens the lymphocytes, equipped by the receptors recognizing this antigen, activate and connect with the antigens. The IRM algorithm simulates the mechanism of removing the ineffective cells and their clones with simultaneous recruitment of the new cells. Therefore in solving an optimization problem the sought optimal solution plays the role of antigen, the values of objective function in obtained partial solutions are considered as the antibodies and the algorithms works by minimizing the difference between the pattern (antigen) and the antibody.

To initiate the IRM algorithm the following steps must be executed:

1. Data initiation:
   $J(\mathbf{x})$ – minimized function, $\mathbf{x} = (x_1, ..., x_n) \in D$;
   N – number of individuals in one population;
   $[x_{lo}, x_{up}]$ – range of j–th variable of individual $\mathbf{x}$;
   μ - mutation parameter;
   β - narrowing parameter;
   I – number of iterations.
2. Random generation of the initial population of individuals $\mathbf{x}$.
3. Sorting of obtained vectors $\mathbf{x}$ with respect to the increasing values of objective function J. Position i_{rank} of the vector denotes its rating position.

The main part of the IRM algorithm consists of the following steps:

1. Determination of the bonding matrix

$$m_{ij} = \begin{cases} 1 - \dfrac{d(\mathbf{x}^i, \mathbf{x}^j)}{d^*} & \text{when } d(\mathbf{x}^i, \mathbf{x}^j) \le d^*, \\ 0 & \text{when } d(\mathbf{x}^i, \mathbf{x}^j) > d^*, \end{cases}$$

   where $d(\mathbf{x}^i, \mathbf{x}^j)$ denotes the distance between individuals $\mathbf{x}^i$ and $\mathbf{x}^j$, and $d^* = d(\mathbf{x}^{best}, \mathbf{x}^{worst})$.
2. Calculation of the stimulation level for each lymphocyte

$$\sigma_j = \sum_{i=1}^{\bar{N}} m_{ij} J(\mathbf{x}^i),$$

   where $\bar{N}$ denotes the fixed (decreasing in time) part of the best lymphocytes.
3. Determination of the threshold value

$$\tau = \frac{1}{\bar{N}} \sum_{i=1}^{\bar{N}} J(\mathbf{x}^i).$$

4. Each individual for which $\sigma_i > \tau$ is mutated according to formula

$$\hat{x}_j^i = x_j^i + \mu_j^i \cdot x_j^i, \qquad j = 1, ..., n,$$

   where $\mu_j^i \in [-\mu, \mu]$ and is randomly generated. In case when the solution is not improved in the assumed number of successive iterations, the new value of mutation parameter, equal to $\beta \cdot \mu$, is taken.
5. New lymphocyte $\hat{\mathbf{x}}$ is added to the population and the worst one is removed.
6. Points 1-5 are repeated I times.

5. NUMERICAL EXAMPLE

To illustrate the investigated procedure we show the solution of the following problem. We consider

the cast of length 0.4 m ($d_0 = 0.4$) solidifying within the mould of length 0.2 m ($b = 0.6$). The parameters describing the process take the following values: $J = 390000$ [J/kg], liquidus and solidus temperatures $T_L = 926$ [K] and $T_S = 886$ [K], temperature of environment $T_\infty = 300$ [K], initial temperature of the solidifying cast $T_0 = 960$ [K], initial temperature of the casting mould $T_{m,0} = 590$ [K] and thermal conductivity of the air gap $\lambda_g = 15$. Moreover, in the liquid phase we have: $c_l = 1275$ [J/(kg·K)], $\rho_l = 2498$ [kg/m^3], $\lambda_l = 183$ [W/(m·K)], in the solid phase we have: $c_s = 1077$ [J/(kg·K)], $\rho_s = 2824$ [kg/m^3], $\lambda_l = 183$ [W/(m·K)] and in the mould we take: $c_m = 620$ [J/(kg·K)], $\rho_l = 7500$ [kg/m^3], $\lambda_m = 40$ [W/(m·K)].

Value of the heat transfer coefficient is unknown and goal of the procedure is to retrieve it. In order to assess the correctness of the method we know the exact value of the reconstructed parameter $\alpha = 250$ [W/m^{2}K]. Additionally, we used this exact value of the sought coefficient to generate the measurement values of temperature for the control point located in the middle of the mould (that is at point 0.5 [m]). However, to avoid the inverse crime (Ryfa & Bialecki, 2011), for calculating the simulated measurements we used the procedure of solving the direct problem but for different mesh (of much bigger density) than by solving the final inverse problem. In this way we have created 12 series of measurement values: perturbed by 0%, 1% and 2% error and read at every 1s, 5s, 10s and 20s.

For solving the direct solidification problem we used the finite difference method combined with the procedure of correcting the temperature field in the vicinity of liquidus and solidus curves. We applied this procedure for the mesh consisted of 500 nodes in the cast region and 150 nodes in the mould region. The implicit difference scheme was executed with respect to the time variable. Step for the time interval was equal to 0.5 s.

For minimizing functional (19) we used the IRM algorithm launched for the following values of parameters: number of individuals $N = 20$, number of iterations $I = 50$, mutation parameter $\mu = 0.9$ and narrowing parameter $\beta = 0.4$. Each individual in our approach represents the value of sought coefficient α. The initial population of the individuals were randomly selected from interval [100,400]. And because of the heuristic nature of the IRM algorithm (meaning that every execution of the procedure can give slightly different result), we calculations were performed 10 time for each set of input data. Thanks to this we could observe the behavior of the examined procedure with respect to the stability of obtained results.

In figure 2 there is displayed the distribution of relative error of the heat transfer coefficient reconstruction in dependence on the number of iterations in IRM algorithm. This is the result of executing the procedure for the cycle of measurements noised by 1% error and taken at every 20 s. We can observe that the error decreases fast and quite quickly we reach the satisfying low value of this error. The calculations are however continued for ensuring the correctness of the final result. The slight increase of the error, observed in the figure, is caused by the fact that by solving the inverse problem the initial data are noised and the reconstructed temperature adjusts to the noised measured temperature once better, once worse leading to such slightly accidental behavior. The procedure is terminated after 50 iteration, because next iterations do not improve significantly the results, only extend the time of calculations.

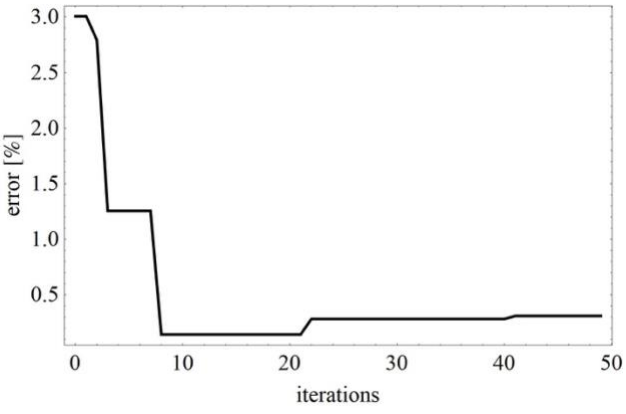

***Fig. 2**. Dependence between the relative error of the heat transfer coefficient reconstruction obtained for the cycle of measurements noised by 1% error and taken at every 20 s and the number of iterations in IRM algorithm.*

Table 1 includes the best obtained values of the reconstructed heat transfer coefficient together with the relative errors and standard deviations of these reconstructions obtained for all considered sets of input data. The relative errors are in each case of the perturbed input data lower than the input data error, only in case of the unburdened input data the error is

higher than zero, however it is not surprising, since the obtained results are just the approximate results. In case of measurements read at every 5s and at every 10s we observe additionally that the reconstruction error obtained for 1% input data error is worse than the error obtained for 2% input data error. It may be explained by the mentioned above fact that the minimized functional (19) is constructed on the basis of perturbed measurement data and it may happen that the reconstructed temperature adapt to the benchmark values once better, once worse. Values of the standard deviations are small, which means that in all considered cases we received similar results. In table 1 there are also collected the maximal absolute and relative errors of the temperature reconstruction. The conclusion is similar: in all cases of considered sets of input data the errors of temperature reconstruction are lower than the input data errors. Summarizing we may state that the noise of measurement values as well as the frequency of measurements do not influence significantly the quality of results.

Table 1. *Best obtained values of the reconstructed heat transfer coefficient ($\overline{\alpha}$), relative errors (δ_α) and standard deviations (S_α) of these reconstructions, together with the maximal absolute ($\Delta_T^{\max}$) and relative ($\delta_T^{\max}$) errors of the temperature reconstruction in control point obtained for the various collections of input data.*

measuments	error [%]	$\overline{\alpha}$ [W/m^{2}K]	δ_α [%]	S_α	$\Delta_T^{\max}$ [K]	$\delta_T^{\max}$ [%]
at every 1 s	0	249.85	0.060	0.509	0.111	0.022
	1	250.12	0.049	0.297	0.090	0.017
	2	250.42	0.166	0.266	0.307	0.595
at every 5 s	0	249.98	0.007	0.372	0.013	0.002
	1	249.83	0.068	0.223	0.127	0.025
	2	249.97	0.013	0.248	0.025	0.005
at every 10 s	0	250.03	0.010	0.399	0.019	0.004
	1	250.37	0.150	0.285	0.277	0.054
	2	249.92	0.033	0.074	0.061	0.012
at every 20 s	0	249.93	0.032	0.628	0.061	0.012
	1	250.20	0.079	0.344	0.145	0.028
	2	250.93	0.373	0.248	0.689	0.133

The discussed results collected in table are supported by the graphs displayed in figures 3 and 4. Figure 3 presents the distribution of relative error of the temperature reconstruction obtained for the cycle of measurements noised by 2% error and taken at every 10 s and 20 s. Whereas figure 4 shows the distribution of temperature reconstructed in the control point located in the middle of the mould for the cycle of measurements taken at every 20 s and noised by 2% error. The reconstructed distribution of temperature is compared there with the exact distribution, however both lines cover, therefore one cannot observe any differences between these lines.

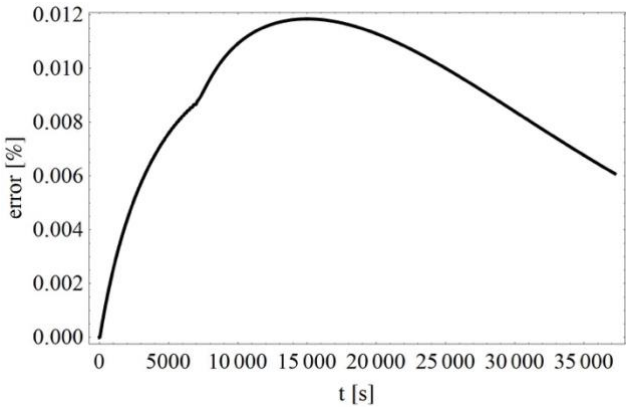

(a)

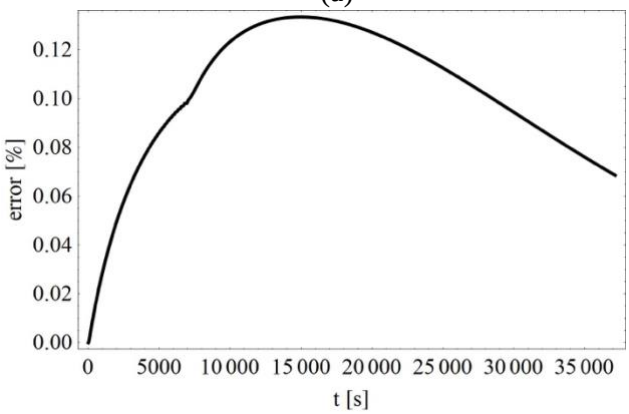

(b)

Fig. 3. *Relative error of the temperature reconstruction obtained for the cycle of measurements noised by 2% error and taken at every 10 s (a) and 20 s (b)*

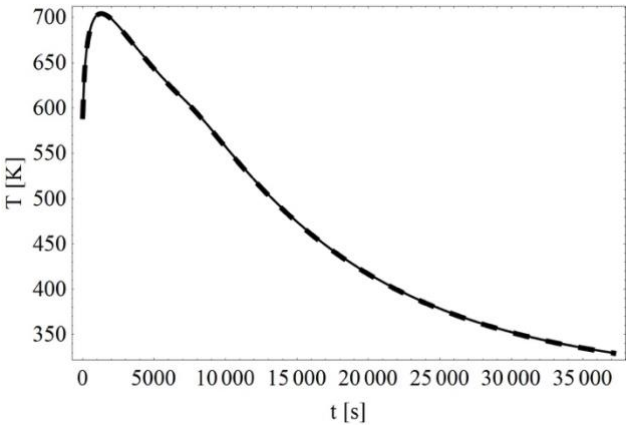

Fig .4. *Distribution of temperature reconstructed in the control point for the cycle of measurements taken at every 20 s and noised by 2% error (solid line – the exact temperature, dashed line – the reconstructed temperature)*

5. CONCLUSIONS

In the paper we investigated the accuracy and usefulness of the approach enabling to solve the inverse one-dimensional solidification problem with the shrinkage of metal included. The process was described by using the model of solidification in the temperature interval, whereas the shrinkage of material was modeled basing on the mass balance equation. And the goal of the inverse problem was to retrieve the value of the unknown heat transfer coefficient together with the distribution of temperature in the cast and in the mould bounding the cast on the ground of the temperature measurements read from the sensor located in the middle of the mould. The procedure of solution was based on two algorithms: the implicit scheme of finite difference method supplemented by the procedure of correcting the field of temperature in the vicinity of liquidus and solidus curves for solving the direct problem and the immune optimization algorithm IRM for minimizing the functional representing the error of approximate distribution of temperature.

The proposed procedure was tested by solving the specific problem on the ground of 12 sets of measurements values. In all considered cases the reconstructions of the sought coefficient and of the temperature were perturbed by the errors lower than the measurement errors and the results obtained in 10 launches of the procedure gave similar results. These observations led as to conclusion that the proposed method of solution works very well, gives satisfactory and stable results.

REFERENCES

Beck, J.V., Blackwell, B., 1988, *Inverse Problems. Handbook of Numerical Heat Transfer*, Wiley Intersc., New York.

Bersini, H., Varela, F., 1991, The Immune Recruitment Mechanism: a selective evolutionary strategy, R. Belew, L. Booker, eds., *Proceedings of the 4th International Conference on Genetic Algorithms*, Morgan Kaufman, San Mateo, 520-526.

Cheung, N., Santos, N.S., Quaresma, J.M.V., G.S. Dulikravich, G.S., Garcia, A., 2009, Interfacial heat transfer coefficients and solidification of an aluminum alloy in a rotary continuous caster, *Int. J. Heat Mass Transfer*, 52, 1-2, 451-459.

Hetmaniok, E., Nowak, I., Słota, D., Zielonka, A., 2012, Determination of optimal parameters for the immune algorithm used for solving inverse heat conduction problems with and without a phase change, *Numerical Heat Transfer B*, 62, 462-478.

Hetmaniok, E., Słota, D., Zielonka, A., 2017, Solution of the direct alloy solidification problem including the phenomenon of material shrinkage, *Thermal Science*, 21, 1A, 105-115.

Hojny, M., Głowacki, M., 2009, The methodology of strain-stress curves determination for steel in semi-solid state, *Arch. Metall. Mater*., 54, 475-483.

Majchrzak, E., Mochnacki, B., 1995, Application of the BEM in the thermal theory of foundry, *Eng. Anal. Bound. Elem*., 16, 2, 99-121.

Mochnacki, B., Suchy, J.S., 1995, *Numerical Methods in Computations of Foundry Processes*, PFTA, Cracow, Poland.

Nawrat, A., Skorek, J., Sachajdak, A., 2009, Identification of the heat fluxes and thermal resistance on the ingot-mould surface in continuous casting of metals, *Inverse Probl. Sci. Eng*., 17, 3, 399-409.

Matlak, J., Słota, D., 2015, Solution of the pure metals solidification problem by involving the material shrinkage and the air-gap between material and mold, *Arch. Foundry Eng*., 15, 47-52.

O'Mahoney, D., Browne, D.J., 2000, Use of experiment and an inverse method to study interface heat transfer during solidification in the investment casting process, *Exp. Therm. Fluid Sci*., 22, 3-4, 111-122.

Piekarska, W., Kubiak, M., Bokota, A., 2011, Numerical simulation of thermal phenomena and phase transformations in laser-arc hybrid welded joint, *Arch. Metall. ater*., 56, 409-421.

Ryfa, A., Bialecki, R., 2011, Retrieving the heat transfer coefficient for jet impingement from transient temperature meaurements, *Int. J. Heat Fluid Flow*, 32, 1024-1035.

Sczygiol, A., Dyja, R., 2007, Evaluating the influence of selectedparameters on sensitivity of a numerical model of solidification, *Archives of Foundry Engineering*, 7(4), 159-164.

Shestakov, N.I., Lukanin, Y.U.V., Kostin, Y.U.P., 1994, Heat exchange regularities in a crystallizer, *Izv. V.U.Z. Chernaya Metall*., 1, 22-23.

Sowa, L., Bokota, A., 2007, Numerical modeling of thermal and fluid flow phenomena in the mould channel, *Archives of Foundry Engineering*, 7(4), 165-168.

Szeliga, D., Gaweda, J., Pietrzyk, M., 2004, Parameters identification of material models based on the inverse analysis, *Int. J. Appl. Math. Comput. Sci*., 14, 549-556.

Talar, J., Szeliga, D., Pietrzyk, M., 2002, Application of genetic algorithm for identification of rheological and friction parameters in copper deformation process, *Arch. Metallurgy*, 47, 27-41.

Telejko, T., Malinowski, Z., 2004, Application of an inverse solution to the thermal conductivity

identification using the finite element method, *J. Mater. Process. Technol.*, 146 (2), 145-155.

Zielonka, A., Hetmaniok, E., Słota, D., 2017, Inverse alloy solidification problem including the material shrinkage phenomenon solved by using the bee algorithm, *Int. Comm. Heat Mass Transf.*, 87, 295-301.

ZASTOSOWANIE ALGORYTMU IMMUNOLOGICZNEGO IRM DO ROZWIĄZANIA ODWROTNEGO ZADANIA KRZEPNIĘCIA STOPU METALI Z UWZGLĘDNIENIEM ZJAWISKA SKURCZU

Streszczenie

W pracy zdefiniowany jest model matematyczny odwrotnego jednowymiarowego zagadnienia krzepnięcia stopu metali z uwzględnieniem zjawiska skurczu. Proces ten jest opisany przy użyciu modelu krzepnięcia w przedziale temperatur, natomiast skurcz metalu zamodelowano na podstawie równania bilansu masy. Zagadnienie odwrotne polega na odtworzeniu współczynnika wnikania ciepła na brzegu formy graniczącym z otoczeniem. Brak tych danych zrekompensowany jest pomiarami temperatury w punkcie kontrolnym zlokalizowanym wewnątrz formy. Metoda rozwiązania rozważanego zagadnienia oparta jest na dwóch procedurach: na schemacie jawnym metody różnic skończonych uzupełnionym procedurą poprawy pola temperatury w sąsiedztwie krzywych liquidus i solidus oraz na algorytmie immunologicznym IRM.

Received: December 20, 2017
Received in a revised form: January 28, 2018
Accepted: February 6, 2018